BIOCHEMISTRY
including biophysical chemistry & molecular biology
Article

Biochemistry **2009,** *48,* 5899–5907 5899
DOI: 10.1021/bi900599s

Chemical Mechanism of Saccharopine Reductase from *Saccharomyces cerevisiae*[†]

Ashwani Kumar Vashishtha, Ann H. West, and Paul F. Cook*

Department of Chemistry and Biochemistry, University of Oklahoma, 620 Parrington Oval, Norman, Oklahoma 73019

Received April 7, 2009; Revised Manuscript Received May 18, 2009

ABSTRACT: Saccharopine reductase (SR) [saccharopine dehydrogenase (L-glutamate forming), EC 1.5.1.10] catalyzes the condensation of L-α-aminoadipate-δ-semialdehyde (AASA) with L-glutamate to give an imine, which is reduced by NADPH to give saccharopine. An acid−base chemical mechanism has been proposed for SR on the basis of pH−rate profiles and solvent deuterium kinetic isotope effects. A finite solvent isotope effect is observed indicating that proton(s) are in flight in the rate-limiting step(s) and likely the same step is limiting under both limiting and saturating substrate concentrations. A concave upward proton inventory suggests that more than one proton is transferred in a single transition state, likely a conformation change required to open the site and release products. Two groups are involved in the acid−base chemistry of the reaction. One of these groups catalyzes the steps involved in forming the imine between the α-amine of glutamate and the aldehyde of AASA. The group, which has a pK_a of about 8, is observed in the pH−rate profiles for V_1 and V_1/K_{Glu} and must be protonated for optimal activity. It is also observed in the V_2 and V_2/K_{Sacc} pH−rate profiles and is required unprotonated. The second group, which has a pK_a of 5.6, accepts a proton from the α-amine of glutamate so that it can act as a nucleophile in forming a carbinolamine upon attack of the carbonyl of AASA.

L-Lysine is biosynthesized by the α-aminoadipate (AAA)[1] pathway in euglenoids and higher fungi such as basidiomycetes, and it is thus a potential target for the development of new antifungals (*1*). The presence of the AAA pathway has been reported in *Saccharomyces cerevisiae* (*2*), *Schizosaccharomyces pombe* (*3*), *Penicillium chrysogenum* (*4*), *Neurospora crassa* (*5*), and *Magnoporthe grisea*, which is a plant pathogen (*6*), and human pathogenic fungi including *Candida albicans* (*7*), *Aspergillus fumigatus* (*8*), and *Cryptococcus neoformans* (*7*). The amino acid sequence of saccharopine reductase (SR) is highly conserved in *S. cerevisiae*, *A. fumigatus*, *C. albicans*, and *C. neoformans*. In order to develop mechanism-based inhibitors that may serve as lead compounds for new antifungal drugs, the kinetic and chemical mechanisms of the enzyme must be known.

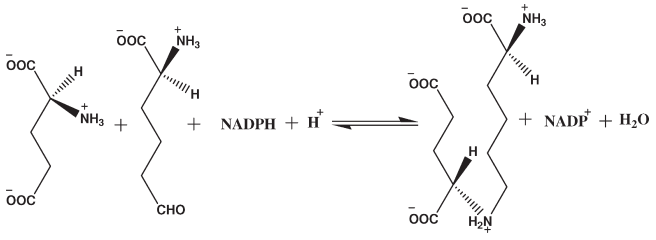

The reductase [saccharopine dehydrogenase (L-glutamate forming), EC 1.5.1.10] catalyzes the penultimate step in the AAA pathway in yeast, the condensation of L-α-aminoadipate-δ-semialdehyde with L-glutamate to give an imine, which is reduced by NADPH to give saccharopine (*6*). Histidine-tagged SR from *S. cerevisiae* has been overexpressed in *Escherichia coli* and purified to about 98% using a Ni-NTA resin (*9*). An ordered kinetic mechanism has been proposed for SR on the basis of initial velocity studies in the absence and presence of product and dead-end inhibitors (*10*). The reduced dinucleotide substrate binds to enzyme first followed by L-α-aminoadipate-δ-semialdehyde (AASA), which adds in rapid equilibrium prior to L-glutamate; saccharopine is released prior to NADP. The pH optimum of SR from *S. cerevisiae* in the physiological reaction direction is 7.0 (*11*), while it is 9.5−9.75 in the direction of semialdehyde formation (*11*, *12*).

Recently, a chemical mechanism was proposed for saccharopine dehydrogenase (SDH) (L-lysine forming) from *S. cerevisiae*, an enzyme that catalyzes a chemical reaction identical to that of the reductase, oxidative deamination of saccharopine, but at an adjacent bond (*16*). The structures of the two enzymes are

[†]This work was supported by the Grayce B. Kerr Endowment to the University of Oklahoma (to P.F.C.) and a grant (GM 071417) from the National Institutes of Health (to P.F.C. and A.H.W.).

*Corresponding author. E-mail: pcook@ou.edu. Tel: 405-325-4581. Fax: 405-325-7182.

[1]Abbreviations: AAA, α-aminoadipate pathway; SR, saccharopine reductase (saccharopine dehydrogenase: L-glutamate forming); NADP, nicotinamide adenine dinucleotide phosphate (the + charge is omitted for convenience); NADPH, nicotinamide adenine dinucleotide phosphate (reduced form); Mes, 2-(*N*-morpholino)ethanesulfonic acid; Mops, 3-(*N*-morpholino)propanesulfonic acid; Ches, 2-(*N*-cyclohexylamino)ethanesulfonic acid; Hepes, 4-(2-hydroxyethyl)-1-piperazineethanesulfonic acid; DCl, deuterium chloride; NaOD, sodium deuterioxide; D_2O, deuterium oxide; SEM, standard error of the mean.

 Published on Web 05/18/2009

dissimilar (*5*, *9*, *34*), and it is thus of interest to determine the chemical mechanism of SR, which has a different regiochemistry compared to SDH. In this paper, we present a detailed analysis of the pH dependence of the kinetic parameters and solvent kinetic deuterium isotope effects of the saccharopine reductase. This is the first report of an acid−base chemical mechanism of a saccharopine reductase.

MATERIALS AND METHODS

Chemicals and Enzymes. L-Saccharopine and L-glutamic acid were from Sigma. β-NADPH and β-NADP were purchased from USB. Mes, Mops, Ches, and Hepes were obtained from Research Organics. Deuterium oxide (99 atom % D) was purchased from Cambridge Isotope Laboratories, Inc. All other chemicals were of the highest grade available and were used as purchased.

Cell growth, expression, and SR purification were carried out as reported previously (*10*).

Enzyme Assay. The SR reaction was monitored by the appearance or disappearance of NADPH at 340 nm (ε_{340}, 6220 M^{-1} cm^{-1}) using a Beckman DU-640 spectrophotometer. All assays were carried out in 500 μL total volume containing 200 mM buffer and appropriate concentrations of substrates. The reaction was initiated by adding 10 μL of appropriately diluted enzyme (0.07−0.12 μM final concentration), and all enzyme dilutions were made fresh for each set of experiments. All assays were carried out at 25 °C.

Initial Velocity Studies at pH 9.0. In order to determine whether the kinetic mechanism changes with pH, initial rate studies were carried out in the direction of formation of L-glutamate at pH 9.0. Initial rate data were collected as a function of NADP (0.02−0.5 mM) at different fixed concentrations of saccharopine (0.1−20 mM).

Inhibition Studies. Product and dead-end inhibition studies were carried out at pH 9.0 by measuring the initial velocity with fixed substrates equal to their respective K_m values and varying the concentration of one substrate around its K_m value (0.5−5K_m) at different fixed concentrations of the inhibitor including zero. First, an estimate of the inhibition constant of an inhibitor was obtained by measuring the initial rate as a function of the inhibitor concentration with all substrates fixed at their respective K_m values. The apparent K_i was then calculated from a plot of $1/v$ vs I with the apparent K_i value equal to the abscissa intercept. Product inhibition patterns were obtained using NADPH as a product inhibitor vs NADP and saccharopine. Glyoxylate was chosen as a dead-end analogue of saccharopine, and dead-end inhibition patterns were obtained for glyoxylate vs saccharopine and NADP.

pH Studies. The pH dependence of V and V/K for all reactants in both reaction directions was obtained by measuring the initial rate as a function of one reactant with all others maintained at saturation ($\geq 10K_m$ unless otherwise specified). The pH was maintained using the following buffers for the pH range indicated at a final concentration of 200 mM: Mes, 5.0−6.5; Mops, 6.5−7.5; Hepes, 7.5−8.5; Ches, 8.0−10.5. The pH was measured before and after the reaction, and no significant change in pH was detected. In order to ensure that no effects of buffer were observed, data were obtained at the same pH when buffers were changed; no effects were observed. The enzyme is stable when incubated for at least 15 min over the pH range 5.0−10.5.

Solvent Deuterium Kinetic Isotope Effects. Initially, the pH and pD dependence of the kinetic parameters was measured, and the isotope effect was estimated as the ratio of the pH(D)-independent values. Solvent kinetic deuterium isotope effects were then measured by direct comparison of initial rates in H_2O and D_2O in the pH(D)-independent range of the pH(D)−rate profiles (8.5−9.5). $^{D_2O}V_2$ and $^{D_2O}(V_2/K_{Sacc})$ were obtained by measuring the rate as a function of saccharopine (0.5−5K_m) with NADP maintained at saturation (10K_m). All substrates and buffers were initially dissolved in a small amount of D_2O and lyophilized to dryness. The dried substrates and buffers were then redissolved in D_2O to give the desired concentrations. The buffers were titrated to the desired pD using DCl or NaOD. The pD value was obtained by adding 0.4 to the pH meter reading (*13*, *17*).

Proton Inventory. In the direction of glutamate formation, finite solvent deuterium kinetic isotope effects were observed, and proton inventory experiments were carried out to measure the solvent deuterium kinetic isotope effects more accurately and estimate the number of proton(s) in flight in the rate-determining transition state(s) (*35*). V_1/K_{Glu} was measured at pH(D) 7.0 in 100% H_2O, 20% D_2O, 40% D_2O, and 85% D_2O with glutamate as the variable substrate at fixed concentrations of NADPH (10K_m) and AASA (5K_m).

Effect of Solvent Viscosity. In order to determine whether the finite solvent deuterium isotope effect included an effect of increased solvent viscosity, 9% glycerol (w/v) was used as the viscosogen, which generates the same relative viscosity as 100% D_2O at 25 °C (*35*). For viscosity dependence studies with L-glutamate as a substrate, the V and V/K for L-glutamate were measured in the absence of glycerol and in the presence of 9% glycerol as a viscosogenic agent.

Primary Kinetic Deuterium Isotope Effects. The initial rate was measured as a function of L-glutamate with NADH(D) and α-AASA maintained at 0.7 mM (0.3K_m) and 10K_m, respectively. Saturation by NADH was not achieved, so the isotope effect on V/K_{Glu} was the only effect measured. All isotope effects were measured in triplicate, and the SEM is reported.

Data Analysis. Initial velocity data obtained in both reaction directions were fitted to eqs 1 and 2 using the Enzfitter program from BIOSOFT, Cambridge, U.K., and programs developed by Cleland (*14*). Initial velocity data at pH 9.0 were fitted to eq 3.

$$v = \frac{VA}{K_a + A} \tag{1}$$

$$v = \frac{VAB}{K_{ia}K_b + K_bA + K_aB + AB} \tag{2}$$

$$v = \frac{VAB}{K_{ia}K_b + K_bA + K_aB + AB\left(1 + \frac{B}{K_{IB}}\right)} \tag{3}$$

In eqs 1, 2, and 3, v and V are the observed initial rate and the maximum rate, respectively, A and B are substrate concentrations, K_a and K_b are Michaelis constants for substrates A and B, respectively, K_{ia} is the dissociation constant for the EA complex, and K_{IB} is the substrate inhibition constant for B.

pH−rate profiles were generated by plotting log V/E_t and log V/KE_t values as a function of pH to assess data quality and to determine the appropriate rate equation for data fitting. pH−rate profiles that exhibited a slope of 1 at low pH and −1 at high pH were fitted using eq 4, while those that exhibited a slope of 1 at low pH were fitted using eq 5. pH−rate profiles with a

slope of 1 at low pH and a slope of −2 at high pH were fitted by using eq 6 or 7.

$$\log y = \log\left[C/\left(1 + \frac{H}{K_1} + \frac{K_2}{H}\right)\right] \quad (4)$$

$$\log y = \log\left[C/\left(1 + \frac{H}{K_1}\right)\right] \quad (5)$$

$$\log y = \log\left[C/\left(1 + \frac{H}{K_1} + \frac{K_2}{H} + \frac{K_2K_3}{H^2}\right)\right] \quad (6)$$

$$\log y = \log\left[C/\left(1 + \frac{H}{K_1} + \frac{{K_0}^2}{H^2}\right)\right] \quad (7)$$

In eqs 4−6, y is the observed value of the parameter (V or V/K) as a function of pH, C is the pH-independent value of y, H is the hydrogen ion concentration, K_1, K_2, and K_3 represent acid dissociation constants for functional groups on the reactant or enzyme required in a given protonation state for optimal binding and/or catalysis, and K_0 is an average value for two acid dissociable groups.

The proton inventory data were fitted using the form of the Gross−Butler equation given in eq 8 (*35*).

$${}^{n}k = {}^{D_2O}k(1 - n + n\phi^{T})^2 \quad (8)$$

In eq 8, ${}^{n}k$ is the ratio of the rate constants (V or V/K) measured in different fractional concentrations of D_2O compared to 100% D_2O, ${}^{D_2O}k$ is the solvent deuterium isotope effect, i.e., the ratio of the rate constants in 100% H_2O and 100% D_2O, n is the fractional concentration of D_2O, and ϕ^T is the fractionation factor for protons of import in the transition state.

RESULTS

Initial Velocity Studies at pH 9.0. In order to determine whether the kinetic mechanism depends on pH, initial velocity patterns were obtained at pH 9.0. In the direction of glutamate formation the initial rate was measured as a function of saccharopine at different fixed concentrations of NADP. An intersecting pattern was obtained. Substrate inhibition by saccharopine is observed that is uncompetitive vs NADP. Data were fitted to eq 3, and estimates of kinetic parameters are summarized in Table 1.

Product inhibition by NADPH is competitive vs NADP and noncompetitive vs saccharopine, consistent with addition of the cofactor to free enzyme. Glyoxylate is competitive vs saccharopine and uncompetitive vs NADP, consistent with the ordered mechanism reported previously (*10*). Inhibition constants are summarized in Table 2.

pH Dependence of Kinetic Parameters. The pH dependence of kinetic parameters provides information on groups required in a given protonation state for optimum binding of reactant and/or catalysis (*17*). The pH dependence of kinetic parameters of the SR reaction was determined, and the results are shown in Figures 1 and 2. In the direction of saccharopine formation, V_1/E_t exhibits a slope of +1 at low pH with a pK_a of 5.7 and decreases at high pH with a pK_a of 7.9 (Figure 1A). NADPH is the first reactant bound in an ordered mechanism, and V_1/KE_t is the on-rate constant for NADPH binding to enzyme. The pH dependence of V_1/K_{NADPH} reflects groups important for binding the dinucleotide. The pH−rate profile has limiting slopes of +1 and −2, giving pK_a values of 6 on the acidic side and an average pK_a of 8.2 on the basic side (Figure 1B). The group with a pK_a of 6 likely reflects the 2′-phosphate of NADPH, which must be ionized for optimum binding (*36*). The group with an average pK_a of 8.2 likely represents an enzyme group that must be protonated for optimum binding of the dinucleotide, probably interacting with the 2′-phosphate and the group observed in the V_1/E_t pH−rate profile; i.e., the protonation state of a catalytic group affects the binding of the nucleotide substrate. The V_1/KE_t for glutamate exhibits a slope of −2 at high pH, giving pK_as of 7.8 and 8.5 and a slope of 1 on the acid pH side with a pK_a of 5.6. The pK_a of 7.8 likely reflects the same enzyme side chain observed in the V_1/E_t pH−rate profile important for catalysis and/or binding, and this will be considered in detail in the Discussion section. pK_a values are summarized in Table 3. Estimates of the pH-independent values of the kinetic parameters are as follows: V_1/E_t, 1.9 ± 0.1 s^{-1}, $V_1/K_{NADPH}E_t$, (7.1 ± 0.5) × 10^4 M^{-1} s^{-1}, and $V_1/K_{Glu}E_t$, (52 ± 5) M^{-1} s^{-1}.

In the direction of AASA formation, V_2/E_t decreases at low pH with a limiting slope of +1, giving pK_a value of 7.2 (Figure 2A). $V_2/K_{NADP}E_t$ decreases at high and low pH with limiting slopes of −1 and +1, giving pK_a values of 10.6 and 6.2 (Figure 2B). $V_2/K_{Sacc}E_t$ also decreases at low and high pH, giving pK_a values of 7.6 and 9.9 (Figure 2C). pK_a values are summarized in Table 3. The pH-independent values of kinetic parameters are as follows: V_2/E_t, 7.8 ± 0.4 s^{-1}, $V_2/K_{NADP}E_t$, (2.0 ± 0.2) × 10^4 M^{-1} s^{-1}, and $V_2/K_{Sacc}E_t$, (2.9 ± 0.5) × 10^4 M^{-1} s^{-1}.

Primary Kinetic Deuterium Isotope Effects with NADH as Slow Substrate. The primary deuterium kinetic isotope effects

Table 1: Kinetic Parameters for SR in the Direction of AASA Formation at pH 7.0 and 9.0

	pH 9	pH 7[a]
V_2/E_t (s^{-1})	13 ± 1	1.06 ± 0.02
$V_2/K_{NADP}E_t$ (M^{-1} s^{-1})	(8.5 ± 1.2) × 10^4	(5.67 ± 0.01) × 10^3
$V_2/K_{Sacc}E_t$ (M^{-1} s^{-1})	(1.7 ± 0.3) × 10^4	(1.6 ± 0.3) × 10^2
K_{NADP} (mM)	0.15 ± 0.01	0.187 ± 0.006
K_{Sacc} (mM)	0.77 ± 0.12	6.6 ± 0.2
K_{iNADP} (mM)	undefined	0.020 ± 0.004
K_{ISacc} (mM)	12 ± 2	

[a] From ref (*10*).

Table 2: Summary of Product and Dead-End Inhibition Data for SR at pH 9.0 in the Direction of AASA Formation

varied substrate	fixed substrate	inhibitor	K_{is} (mM)	K_{ii} (mM)	inhibition pattern obsd
NADP	saccharopine (K_m)	NADPH	0.027 ± 0.001	N/A[a]	C
saccharopine	NADP (K_m)	NADPH	0.12 ± 0.02	0.20 ± 0.03	NC
saccharopine	NADP (K_m)	glyoxylate	14 ± 2	N/A	C
NADP	saccharopine (K_m)	glyoxylate		15 ± 1	UC

[a] N/A is not applicable.

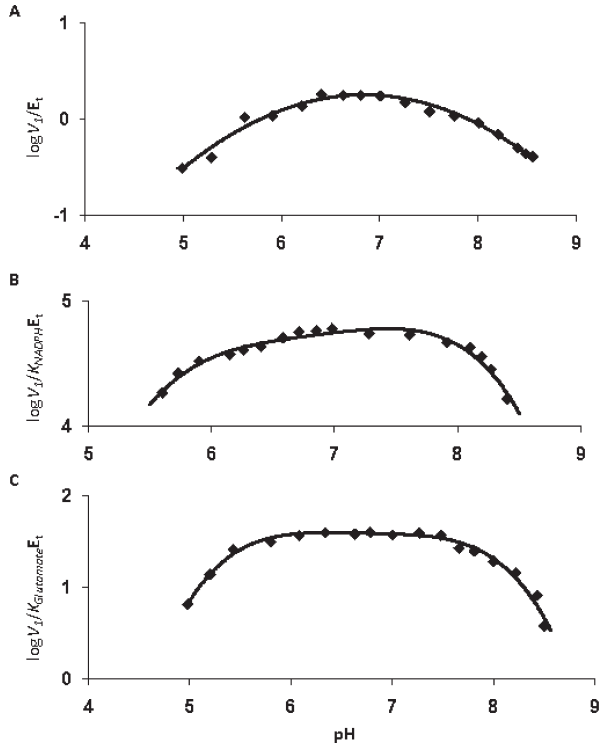

FIGURE 1: pH dependence of kinetic parameters in the direction of saccharopine formation. pH dependence of (A) V_1/E_t, (B) $(V_1/K_{NADPH})E_t$, and (C) $(V_1/K_{Glu})E_t$. All data were obtained at 25 °C. Points are experimental, while curves are based on a fit of the data to eq 4 for (A), eq 7 for (B), or eq 6 for (C).

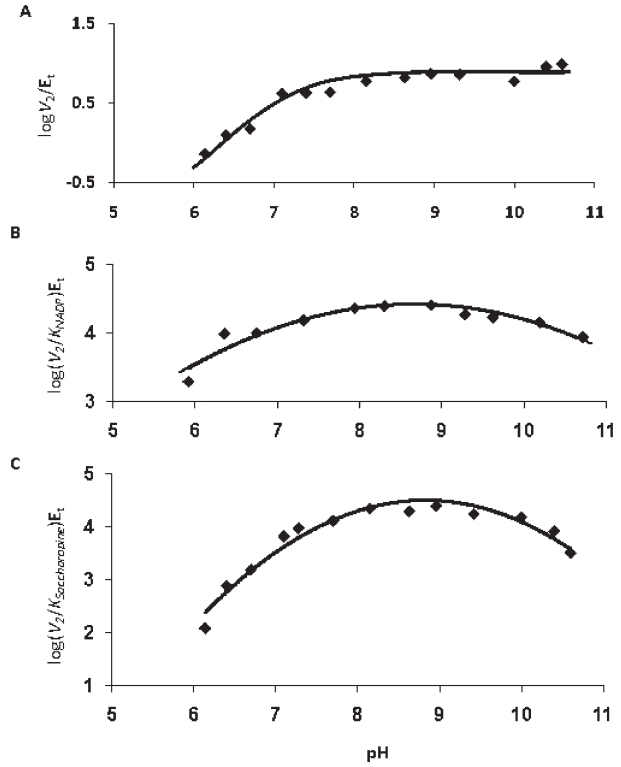

FIGURE 2: pH dependence of kinetic parameters in the direction of glutamate formation. pH dependence of (A) V_2/E_t, (B) $(V_2/K_{NADP})E_t$, and (C) $(V_2/K_{Sacc})E_t$. All data were obtained at 25 °C. Points are experimental, while curves are based on a fit of the data to eq 5 (A) or eq 4 (B, C).

on V and V/K_{Glu}, obtained with NADPH(D), are 1 and 0.87, respectively (*10*). In order to obtain an estimate of the rate of the catalytic steps with the natural substrates, the isotope effect on the hydride transfer step was measured with the slow substrate, NADH(D). An estimate of $V_1/K_{NADH}E_t$ was obtained by measuring the initial rate as a function of NADH concentration with AASA and glutamate fixed at $10K_m$. K_{NADH} is high and saturation was not attained. The $V_1/K_{NADH}E_t$ is (24 ± 0.9) M^{-1} s^{-1}. The ratio of $V_1/K_{NADPH}E_t$ and $V_1/K_{NADH}E_t$ at pH 7.0 is (2.9 ± 0.2) × 10^4. The isotope effect on V_1/K_{Glu} at pH 7.0 is 1.9 ± 0.7.

Effect of Solvent Deuterium and Viscosity. Initial rates were measured at saturating NADP, varying saccharopine over the pH(D) range 6.5−10.5 (Figure 3). Solvent isotope effects were calculated as the ratio of the pH(D)-independent values of V_2 and V_2/K_{Sacc}. Equal values of 1.8 ± 0.1 were obtained for $^{D_2O}V_2$ and $^{D_2O}V_2/K_{Sacc}$.

Glycerol was used as a viscosogen for SR. The ratio of the values of V_1 and V_1/K_{Glu} determined in H_2O and at a relative viscosity of 1.24 are within error equal. Therefore, the values of the observed solvent isotope effects, $^{D_2O}V_2$ and $^{D_2O}(V_2/K_{Sacc})$, result from a classical isotope effect and not from an effect of the increased viscosity of 100% D_2O.

Proton Inventory. A proton inventory is obtained from the change in V/K_{Glu} with the concentration of D_2O. At pH(D) 7.0, the proton inventory is shown in Figure 4. The proton inventory is nonlinear and can be best described as concave upward. A fit of the Gross−Butler equation to the data gives $^{D_2O}k = 1.72 \pm 0.07$, within error equal to that estimated from the pH(D) profiles, and $\phi^T = 0.70 \pm 0.04$ for the two protons in the rate-determining transition state in the reaction catalyzed by SR in the direction of saccharopine formation.

Table 3: Summary of pK_a Values for SR

parameter	pK_1	pK_2	pK_3
	Forward Reaction		
V_1	5.7 ± 0.2	7.9 ± 0.1	
V_1/K_{NADPH}	6.0 ± 0.2	8.2 ± 0.1[a]	
V_1/K_{Glu}	5.6 ± 0.1	7.8 ± 0.1	8.5 ± 0.2
	Reverse Reaction		
V_2	7.2 ± 0.1		
V_2/K_{NADP}	6.2 ± 0.1	10.6 ± 0.1	
V_2/K_{Sacc}	7.6 ± 0.1	9.9 ± 0.2	

[a] Average value.

DISCUSSION

Initial Velocity Studies at pH 9.0. In the direction of saccharopine oxidative deamination, a double reciprocal plot of initial rate vs saccharopine concentration at different fixed levels of NADP exhibits substrate inhibition by saccharopine that is uncompetitive vs NADP. The substrate inhibition suggests binding of saccharopine to the E−NADPH complex, which builds up in the steady state; K_{ISacc} is 12 mM. Substrate inhibition by saccharopine is complete since the initial rate tends to zero as the substrate concentration tends to infinity. Values of $V_2/K_{NADP}E_t$ and $V_2/K_{Sacc}E_t$ are 8.5 × 10^4 M^{-1} s^{-1} and 1.7 × 10^4 M^{-1} s^{-1}, lower than the diffusion-limited rate constant of 10^8−10^9 $M^{-1}s^{-1}$, suggesting diffusion of reactant and enzyme together does not completely limit the reaction.

Product inhibition by NADPH is competitive vs NADP and noncompetitive vs saccharopine, suggesting NADP is the

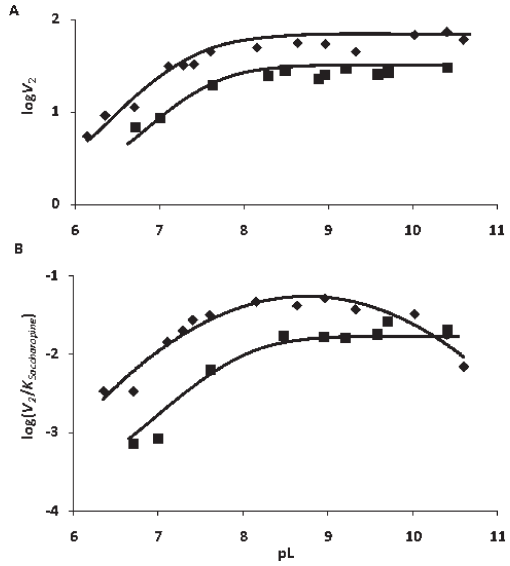

FIGURE 3: pH(D) dependence of V_2/E_t and $(V_2/K_{Sacc})E_t$ at 25 °C in the direction of glutamate formation. (A) V_2/E_t vs pL (pH or pD) in H_2O (◆) and in D_2O (■). (B) $(V_2/K_{Sacc})E_t$ in H_2O (◆) and D_2O (■). Points are experimental, while curves are based on a fit of the data to eq 5 (A) and eq 4 (B).

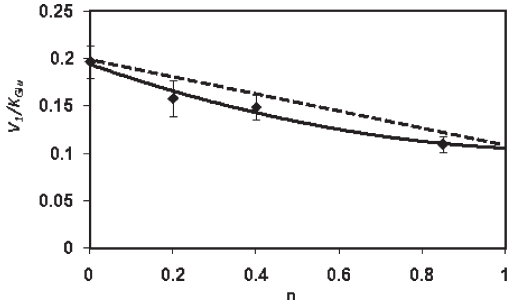

FIGURE 4: Proton Inventory. Dependence of V_1/K_{Glu} on the fraction of deuterium (n) in solvent. Velocities were measured at a pH(D)-independent value of 7.0 in 100% H_2O, 20% D_2O, 40% D_2O, and 85% D_2O. Points are experimental values, and the curve is theoretical on the basis of the fit to eq 8. The dotted line is theoretical for a linear proton inventory.

first substrate to add to enzyme followed by saccharopine, which adds to the E−NADP binary complex. In agreement, glyoxylate, a dead-end analogue of saccharopine, is competitive against saccharopine and uncompetitive vs NADP, indicating binding to the E−NADP complex. Overall, data are consistent with the ordered mechanism reported at pH 7.0 (*10*). As suggested above, the uncompetitive substrate inhibition by sacharopine suggests release of NADPH contributes to rate limitation at pH 9.0 in the direction of glutamate formation. An estimate of the contribution can be obtained from the difference in pK_a values of V_2/E_t and $V_2/K_{Sacc}E_t$. The pK_a observed for $V_2/K_{Sacc}E_t$ is likely close to the intrinsic pK_a for an enzyme side chain (see below, Interpretation of pH Dependence of Kinetic Parameters). The pK_a observed in the V_2/E_t pH−rate profile is perturbed to lower pH by about 0.4 pH unit. The perturbation of the pK_a is dependent on the ratio of the net rate constant of the chemical steps to the rate constant for release of NADPH; app pK_a = pK_a − log(1 + $k_{chem}/k_{offNADPH}$) (*15*). A value of 1.5 is estimated for $k_{chem}/k_{offNADPH}$, suggesting the release of NADPH is 1.5 times slower than the rate of the chemical step. This would give a value of about 8 mM for the K_I for saccharopine substrate inhibition corrected to 100% E−NADPH.

Interpretation of Solvent Deuterium Kinetic Isotope Effects. Isotope effects were previously measured using NADPH(D) in the direction of saccharopine formation (*10*). A value near unity was observed for $^DV_1$, while an inverse effect of about 0.87 was observed for $^D(V_1/K_{Glu})$. Data were interpreted in terms of a slow release of products, including saccharopine. A primary deuterium isotope effect of 1.9 ± 0.7 is estimated on V_1/K_{Glu} using NADH(D). Although not well-defined, a finite normal isotope effect is observed.

Solvent isotope effects probe proton transfer in chemical reactions. As a result, solvent isotope effects were measured for the SR reaction in the direction of AASA formation as the ratio of the pH(D)-independent values in the pH(D)−rate profiles. It is important to note that equilibrium solvent deuterium isotope effects are observed on the pK_a values of acid dissociable groups of oxygen or nitrogen-containing acids and bases that result in an increase in the pK_a by 0.4−0.6 pH unit (*35*). As seen in Figure 3, the expected shift in the pK_a is observed reflecting the equilibrium isotope effect, and in addition, the pH-independent value is lower in D_2O than in H_2O, indicating a kinetic isotope effect. A normal effect of 1.8 is observed on V_2 and V_2/K_{Sacc}. The change in solvent viscosity that results from substitution of D_2O for H_2O can account for solvent isotope effects (*37*, *38*). Kinetic parameters at increased viscosity are identical, within error, to those observed in H_2O, strongly suggesting the isotope effects are not a consequence of the change in solvent viscosity. The finite solvent isotope effect and concave upward proton inventory are consistent with the rate-determining conformational change to open the site and release products. An estimate of the number of protons important to the overall reaction and the number of solvent-derived proton transfer steps that contribute to rate limitation can be obtained from the proton inventory method (*35*). If a single proton is transferred in the rate-limiting transition state, a plot of the rate constant versus atom fraction of deuterium (n) will be linear. If more than one proton is transferred in a single transition state, the plot will be concave upward, while if protons are transferred in multiple transition states, the plot will be concave downward. A concave upward proton inventory is observed for V_1/K_{Glu}, suggesting that more than one proton is transferred in a single transition state. The reaction catalyzed by SR involves two protons and these protons have identical fractionation factors, suggesting equal contributions to the transition state for both protons. (Attempts to fit the data to other forms of the Gross−Butler equation, e.g., allowing the fractionation factors for both protons to be independent, failed.) Data suggest a proton transfer is involved in the rate-limiting step in the reaction. Given the results with NADPH(D), the step(s) must involve the conformational change to open the site and release products.

Interpretation of pH Dependence of Kinetic Parameters. The maximum rate, V, is obtained at saturating concentrations of all substrates, and the dominant enzyme form will depend on the location of the slow step(s). As suggested above, the slow step occurs after the chemical steps and accompanies product release. The V/K for a reactant is obtained at limiting concentrations of one of the reactants and saturating levels of all others, and free substrate and the enzyme form to which the substrate binds are dominant in the steady state. The V profile reflects groups required in a given protonation state for catalysis, while the V/K profile will reflect the protonation state of groups on reactant and/or enzyme responsible in a given protonation state for binding and/or catalysis (*17*). In an ordered

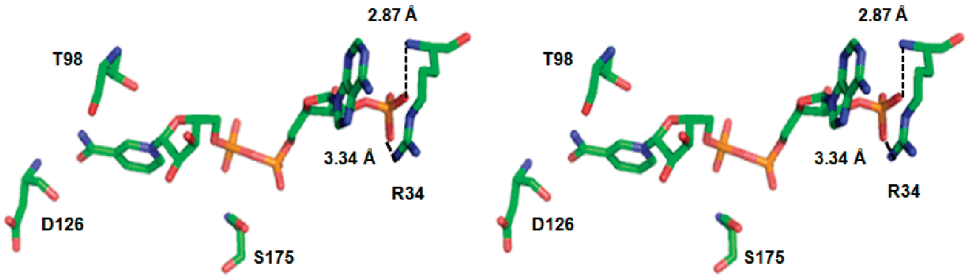

FIGURE 5: Stereoview of a close-up of the saccharopine reductase from the *M. grisea* (PDB code 1E5Q) binding site for NADP(H). Residues that interact with the cofactor and their hydrogen-bonding distances are shown. The following color scheme is used: C, green, O, red, N, blue; and P, orange. This figure was generated using the PyMOL molecular visualization program (Web site: http:// pymol.Sourcefor ge.net/).

mechanism, the V/K for all of the reactants with the exception of the last one to add is the on rate constant for binding reactant to enzyme, and its pH dependence will thus reflect groups important for binding.

In the direction of saccharopine formation, the free enzyme and NADPH predominate for the V_1/K_{NADPH} profile, while E−NADPH−AASA and glutamate predominate for the V_1/K_{Glu} profile. However, AASA adds in rapid equilibrium prior to glutamate, and as a result K_{AASA} is zero and thus a V_1/K_{AASA} profile was not obtained.[2] In the nonphysiologic reaction direction, the free enzyme and NADP predominate for the V_2/K_{NADP} profile, while E−NADP and free saccharopine dominate for the V_2/K_{Sacc} profile, and the enzyme form that precedes the slow step(s) at saturating substrates dominates for the V_2 pH−rate profile.

The V_1/K_{NADPH} exhibits the requirement for a group with a pK_a of 6 that must be unprotonated and two groups with an average pK_a of 8.2 that must be protonated for optimum binding of NADPH. The V_2/K_{NADP} reflects the need for a group with a pK_a of 6.2 that must be unprotonated and a second group with a pK_a of 10.6 required protonated for optimum binding of NADP. The ionization state of the 2′-phosphate of NADP(H) is often an important binding determinant for NADP-dependent enzymes, e.g., as seen for glutathione reductase (*39*). In agreement, the V/K for NADH is 10^4-fold lower than that of NADPH. The pK_a of the 2′-phosphate is 6.1 (*36*), within error identical to the pK_a of 6−6.2 observed in the V_1/K_{NADPH} and V_2/K_{NADP} pH−rate profiles. A group that must be protonated is observed in the pH−rate profile of V_2/K_{NADP}, with pK_a value of 10.6. An arginine (R34) is within hydrogen-bonding distance to the 2′-phosphate of the dinucleotide substrate (Figure 5) (*6*, *9*). The group with a pK_a of 10.6 observed in the V_2/K_{NADP} pH−rate profile may reflect R34, which forms a salt bridge with the 2′-phosphate and is completely conserved in SR amino acid sequences from fungi including *S. cerevisiae* and human pathogenic fungi such as *C. albicans* (*7*), *A. fumigatus* (*8*), and *C. neoformans* (*7*) and the plant pathogen *M. grisea* (*6*). One of the groups with an average pK_a of about 8.2 observed in the V_1/K_{NADPH} pH−rate profile that must be protonated is likely the same group seen in the V_1 and V_1/K_{Glu} pH−rate profiles, and this will be discussed below under Proposed Chemical Mechanism. The function of the second group with a pK_a of 8.2 is not known. If the pH−rate profile could be extended to higher pH, the group with a pK_a of 10.6, thought to reflect R34, should also be observed.

[2]The rate equation for an equilibrium ordered kinetic mechanism is $v = VAB/(K_{ia}K_b + K_bA + AB)$. The lack of a K_a term derives as a result of B at very high concentrations forcing all of the EA into central complexes at any reasonable concentration of A (*15*).

The V_1/K_{Glu} profile exhibits the requirement for groups with pK_as of about 7.8 and 8.5 that must be protonated and a group with a pK_a of 5.6 that must be unprotonated for optimum binding and catalysis. The group with a pK_a of 7.8 is also observed in the V_1 pH−rate profile and likely reflects the catalytic general acid group, which protonates the carbonyl oxygen of AASA as the carbinolamine is formed upon attack by the α-amine of glutamate. In agreement, a group on the enzyme with a pK_a of 7.2−7.6 is observed in the V_2 and V_2/K_{Sacc} pH−rate profiles that must be unprotonated for catalysis in the direction of glutamate formation. In the reverse reaction direction the group activates H_2O as it attacks the imine carbon formed upon oxidation of saccharopine and thus must be unprotonated. In the nonphysiologic reaction direction (formation of glutamate), the observed pK_a in the V_2/K_{Sacc} pH−rate profile is 7.6, probably the intrinsic pK_a for the catalytic group, is perturbed to higher pH in the opposite direction (V_1/K_{Glu} pH−rate profile). It is possible that the group responsible is D125, which is in the vicinity of the saccharopine secondary amine in the structure of the E−NADPH−saccharopine complex of SR from *M. grisea*, a closely related homologue of the *S. cerevisiae* SR (*6*). This residue is completely conserved in SR amino acid sequences from fungi including *S. cerevisiae* and human pathogenic fungi such as *C. albicans* (*7*), *A. fumigatus* (*8*), and *C. neoformans* (*7*).

The group with a pK_a of 5.6, observed in the V_1/K_{Glu} and V_1 pH−rate profiles, is likely a base required to accept a proton from the α-amine of glutamate prior to its nucleophilic attack on the semialdehyde carbonyl. One would also expect to see this group in the V_2/K_{Sacc} pH−rate profile if it could be extended to lower pH, since the same group is responsible for accepting a proton from the saccharopine secondary amine. The identity of this group is at present unknown.

The V_2/K_{Sacc} pH−rate profile exhibits a pK_a of 9.9, while the V_1/K_{Glu} pH−rate profile exhibits a pK_a 8.5. These groups are not observed in V_2 or V_1 pH−rate profiles and thus reflect binding groups for saccharopine and glutamate, respectively. The pK_a value of the secondary amino group of saccharopine is 10.1 (*16*), while the pK_a of the α-amine of glutamate is about 9.5 (*36*). Thus, the additional binding groups likely reflect the substrate amine pK values, suggesting they must be protonated for optimum binding.

It is also possible that substrates bind with their amine unprotonated and that they are in reverse protonation state with an enzyme group; i.e., although the pK_a is observed on the basic side, the group must be unprotonated for optimum binding, while the group observed on the acid side must be protonated (*15*). Data are not in agreement with this suggestion. Reverse protonation may work in the direction of saccharopine formation since pK_a values are observed on the acid and base sides of the V_1/K_{Glu} pH−rate profile and a general acid catalyst is

Scheme 1: Proposed Chemical Mechanism for Saccharopine Reductase[a]

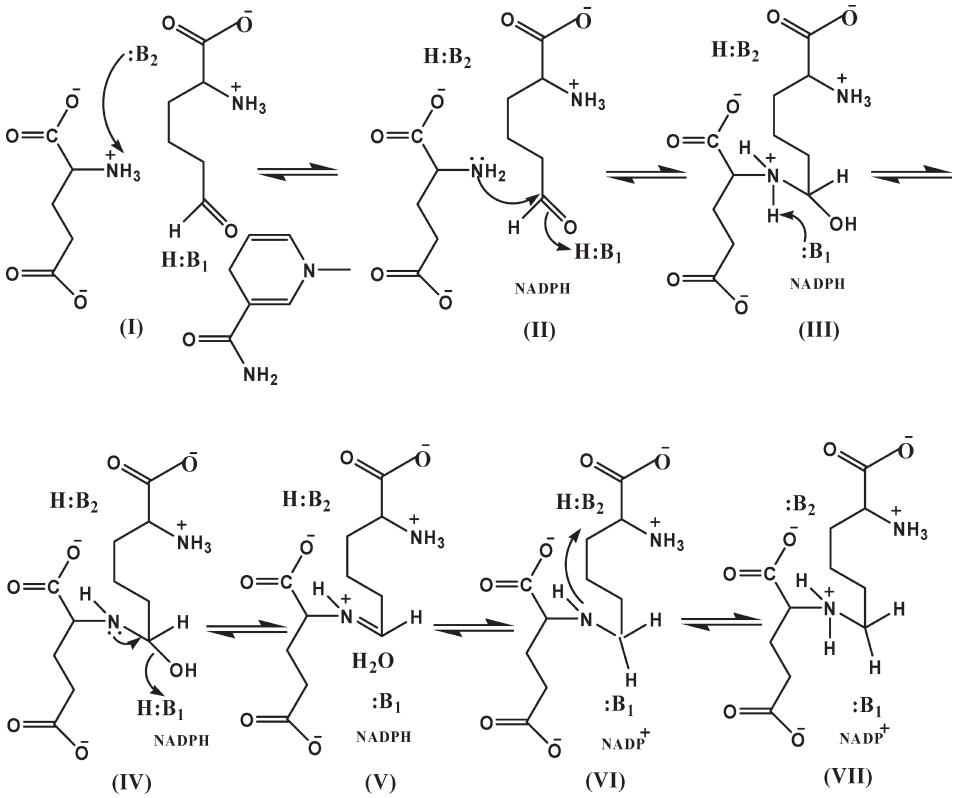

[a] I, the central E−NADPH−AASA−glutamate complex formed upon binding of substrates; II, production of the neutral amine of glutamate, which acts as a nucleophile attacking the carbonyl of the semialdehyde; III, protonated carbinolamine intermediate; IV, neutral carbinolamine intermediate; V, the protonated imine intermediate; VI, neutral L-saccharopine formed upon hydride transfer from NADPH; and VII, protonated saccharopine.

required in this reaction direction. However, in the opposite reaction direction, reverse protonation states would require that the saccharopine secondary amine is unprotonated and the enzyme group is protonated. Since a general base is required in this reaction direction, data are not in agreement with reverse protonation states. Thus, the α-amine of glutamate and the secondary amine of saccharopine must be protonated for appropriate binding and catalysis, and an enzyme group must act as a base to accept a proton prior to reaction. The only group observed on the acid side of the V_1/K_{Glu} pH−rate profile is the one with a pK_a of 5.6.

Proposed Chemical Mechanism of Saccharopine Reductase. On the basis of the pH−rate profiles, an acid−base chemical mechanism is proposed as shown in Scheme 1. The reaction begins with all reactants bound (I), which requires the α-amine of L-glutamate protonated (Figure 6) and NADPH bound with its 2′-phosphate ion paired with R34 on enzyme (Figure 5). As seen in Figure 6, the α-carboxylates of the substrates, L-glutamate and AASA, are within hydrogen bond distance to arginine residues, while the γ-carboxylate of the L-glutamate substrate is within hydrogen bond distance to a tyrosine and serine. An enzyme group with a pK_a of 5.6−5.7, B_2, accepts a proton from the α-amine of glutamate to generate the neutral amine that can act as a nucleophile (II). The α-amine of glutamate attacks the carbonyl of the semialdehyde to generate the carbinolamine, which is protonated by a second enzyme group with a pK_a of about 7.8−8, B_1, which may be D125 (III). The distance between the closest oxygen of D125 and the secondary amine nitrogen of saccharopine is long enough (5.57 Å) to accommodate a water molecule. The protonation state of this group apparently affects the binding of NADPH, but not NADP, since it is observed in the V_1/K_{NADPH} pH−rate profile. The reason for the effect on NADPH binding is not obvious but may reflect optimizing the conformation of the Michaelis complex. A proton is accepted from the carbinolamine (III), to give the neutral carbinolamine (IV), which can then collapse, expelling water with a proton donated by B_1 (V). NADPH reduces the imine, generating the unprotonated secondary amine (VI), which is protonated by B_1 (VII), and saccharopine is released. On the basis of the finite solvent deuterium kinetic isotope effect, the release of saccharopine may be coupled to a conformational change accompanying proton transfer to the secondary amine nitrogen. The proposed mechanism is now being tested using site-directed mutagenesis. An important question is: What is the identity of the general acid that accepts a proton from the α-amine of glutamate?

Comparison to Other NAD(P)-Dependent Oxidative Deaminases. The enzymes that are involved in pyridine nucleotide-dependent oxidative deamination reactions can be roughly divided into two classes, those that carry out the oxidative deamination of primary amines and those that function with secondary amines. Of the primary amine dehydrogenases, glutamate (*18*−*22*) and alanine (*19*, *23*, *24*) dehydrogenases are well studied. However, the closest relative to SR is saccharopine dehydrogenase (SDH), which catalyzes the reaction following that catalyzed by SR and results in the formation of lysine and saccharopine. Indeed, the reaction chemistry is identical and occurs at a C−N bond adjacent to the C−N bond formed by SR (*1*). The SDH from *S. cerevisiae* was the only secondary amine dehydrogenase that has been characterized with respect to its

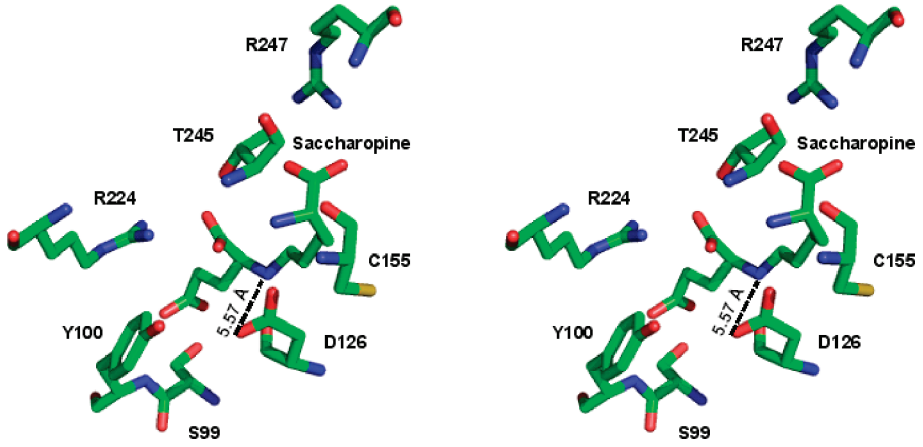

FIGURE 6: Stereoview of a close-up of the active site of saccharopine reductase from *M. grisea* (PDB code 1E5Q). Residues that interact with saccharopine and their hydrogen-bonding distances are shown. Colors are as in the legend to Figure 5. This figure was generated using the PyMOL molecular visualization program.

chemical mechanism prior to this study (*16*, *25*−*27*). The mechanism of the closely related SDH will be considered first.

Saccharopine is a common substrate for the last two enzymes of the AAA pathway, and as suggested above, SR and SDH differ in their regiochemistry. In spite of the two enzymes having virtually no identity in their primary, secondary, and tertiary structure (*9*, *34*), they catalyze the same reaction. Both enzymes utilize the same general acid−base catalytic strategy to catalyze their reaction. Beginning with saccharopine and NAD(P), the enzymes both utilize two bases to catalyze the reaction. In both cases the secondary amine of saccharopine must be protonated for optimum binding and reaction, as is true for the α-amine of glutamate (SR) and the ε-amine of lysine (SDH). A second base carries out most of the chemistry in both cases, i.e., beginning with sacchaopine, hydrolysis of the imine formed upon oxidation. The identity of the catalytic groups in SDH has not yet been determined, but there is no paucity of groups in the active site and in proximity to reactants that can serve in this capacity. On the other hand, there are no obvious candidates, other than D125, that can serve as a catalyst in the active site of SR. In addition, chemistry contributes to rate limitation in SDH, while product release limits the SR reaction.

α-Amino acid dehydrogenases, such as glutamate and alanine dehydrogenase, generate ammonia, a α-keto acid, and reduced pyridine dinucleotide as products of the oxidative deamination reaction (*28*). The glutamate dehydrogenases (GDH) from bovine liver and *Chlorella sorokiniana* have been studied, and an acid−base chemical mechanism has been proposed on the basis of pH−rate and pK_i profiles (*29*, *30*). Chemical mechanisms of other amine dehydrogenases, including alanine dehydrogenase from *Bacillus subtilis* (*31*), L-phenylalanine dehydrogenase from *Rhodococcus* sp. M4 (*32*), and leucine dehydrogenase from *Bacillus stearothermophilus* (*33*), have also been studied.

The chemical mechanisms of the above primary amine dehydrogenases are very similar to one another. They all employ general acid−base catalysis, and the chemical mechanisms are similar overall and very similar to the strategy utilized by the secondary amine dehydrogenases. The main difference between the two classes of dehydrogenase is the protonation state of the α-amine of the substrate, glutamate or alanine. The secondary amine dehydrogenases bind saccharopine with its secondary amine protonated, while the primary amine dehydrogenases selectively bind reactant with a neutral amine (*29*, *31*). Oxidation generates the protonated imine, which is attacked by water, activated by an active site lysine. The same group then functions to generate the ammonia and ketone products. The neutral ammonia is then released, opposed to the protonated α-amine of glutamate or lysine in the secondary amine dehydrogenases. Another difference in the primary amine dehydrogenases is the identity of the acid−base catalyst. L-Glutamate (*29*) and phenylalanine (*32*) dehydrogenases utilize a lysine as the base, while alanine dehydrogenase uses a histidine (*31*). The identity of the base may also differ in the secondary amine dehydrogenases, but this will have to await additional studies that are now in progress.

ACKNOWLEDGMENT

We thank Dr. William E. Karsten and Dr. Babak Andi for cloning the gene encoding SR from *S. cerevisiae*.

REFERENCES

(1) Xu, H., Andi, B., Qian, J., West, A. H., and Cook, P. F. (2006) The α-aminoadipate pathway for lysine biosynthesis in fungi. *Cell Biochem. Biophys. 46*, 43–64.
(2) Broquist, H. P. (1971) Lysine biosynthesis (yeast). *Methods Enzymol. 17*, 112–129.
(3) Ye, Z. H., and Bhattacharjee, J. K. (1988) Lysine biosynthesis pathway and biochemical blocks of lysine auxotrophs of *Schizosaccharomyces pombe*. *J. Bacteriol. 170*, 5968–5970.
(4) Jaklitsch, W. M., and Kubicek, C. P. (1990) Homocitrate synthase from *Penicillium chrysogenum*. Localization, purification of the cytosolic isoenzyme, and sensitivity to lysine. *J. Biochem. 269*, 247–253.
(5) Trupin, J. S., and Broquist, H. P. (1965) Saccharopine, an intermediate of the aminoadipic acid pathway of lysine biosynthesis. I. Studies in *Neurospora crassa*. *J. Biol. Chem. 240*, 2524–2530.
(6) Johansson, E., Steffens, J. J., Lindqvist, Y., and Schneider, G. (2000) Crystal structure of saccharopine reductase from *Magnaporthe grisea*, an enzyme of the α-aminoadipate pathway of lysine biosynthesis. *Structure 8*, 1037–1047.
(7) Garrad, R. C., and Bhattacharjee, J. K. (1992) Lysine biosynthesis in selected pathogenic fungi: characterization of lysine auxotrophs and the cloned *LYS1* gene of *Candida albicans*. *J. Bacteriol. 174*, 7379–7384.
(8) Palmer, D. R., Balogh, H., Ma, G., Zhou, X., Marko, M., and Kaminskyj, S. G. (2004) Synthesis and antifungal properties of compounds which target the alpha-aminoadipate pathway. *Pharmazie 59*, 93–98.
(9) Andi, B., Cook, P. F., and West, A. H. (2006) Crystal structure of His-tagged saccharopine reductase from *Saccharomyces cereviciae* at 1.7 Å resolution. *Arch. Biochem. Biophys. 46*, 243–254.
(10) Vashishtha, A. K., West, A. H., and Cook, P. F. (2008) Overall kinetic mechanism of saccharopine dehydrogenase from *Saccharomyces cerevisiae*. *Biochemistry 47*, 5417–5423.
(11) Storts, D. R., and Bhattacharjee, J. K. (1987) Purification and properties of saccharopine dehydrogenase (glutamate forming) in

Saccharomyces cerevisiae lysine biosynthetic pathway. *J. Bacteriol. 169*, 416–418.
(12) Jones, E. E., and Broquist, H. P. (1966) Saccharopine, an intermediate of the aminoadipic acid pathway of lysine biosynthesis. III. Aminoadipic semialdehyde-glutamate reductase. *J. Biol. Chem. 241*, 3430–3434.
(13) Schowen, K. B., and Schowen, R. L. (1982) Solvent isotope effects on enzyme systems. *Methods Enzymol. 87*, 551.
(14) Cleland, W. W. (1979) Statistical analysis of enzyme kinetic data. *Methods Enzymol. 63*, 103–108.
(15) Cook, P. F., and Cleland, W. W. (2008) Enzyme Kinetics and Mechanism , pp 325−364, Garland Publishing, New York.
(16) Xu, H., Alguindigue, S. S., West, A. H., and Cook, P. F. (2007) A proposed proton shuttle mechanism for saccharopine dehydrogenase from *Saccharomyces cerevisiae*. *Biochemistry 46*, 871–882.
(17) Cleland, W. W. (1977) Determination the chemical mechanisms of enzyme-catalyzed reactions by kinetic studies. *Adv. Enzymol. Relat. Areas Mol. Biol. 45*, 273–387.
(18) Cook, P. F. (1982) Kinetic studies to determine the mechanism of regulation of bovine liver glutamate dehydrogense by nucleotide effectors. *Biochemistry 21*, 113–116.
(19) Weiss, P. M., Chen, C. Y., Cleland, W. W., and Cook, P. F. (1988) Use of primary deuterium and ^{15}N isotope effects to deduce the relative rates of steps in the mechanisms of alanine and glutamate dehydrognases. *Biochemistry 27*, 4814–4822.
(20) Frieden, C. F. (1959) Glutamic dehydrogenase. The order of substrate addition in the enzymatic reaction. *J. Biol. Chem. 234*, 2891–2896.
(21) Engel, P. C., and Dalziel, K. (1970) Kinetic studies of glutamate dehydrogenase. The reductive amination of 2-oxoglutarate. *Biochem. J. 118*, 409–419.
(22) Colen, A. H., Prough, R. A., and Fisher, H. F. (1972) The mechanism of the glutamate dehydrogenase reaction. Evidence for random and rapid binding of substrate and coenzyme in the burst phase. *J. Biol. Chem. 247*, 7905–7909.
(23) Ohshima, T., Sakane, M., Yamazaki, T., and Soda, K. (1990) Thermostable alanine dehydrogenase from thermophilic *Bacillus sphaericus* DSM 462. Purification, characterization and kinetic mechanism. *Eur. J. Biochem. 191*, 715–720.
(24) Grimshaw, C. E., and Cleland, W. W. (1981) Kinetic mechanism of *Bacillus subtilis* L-alanine dehydrogenase. *Biochemistry 20*, 5650–5655.
(25) Fujioka, M., and Nakatani, Y. (1970) A kinetic study of the saccharopine dehydrogenase reaction. *Eur. J. Biochem. 16*, 180–186.
(26) Fujioka, M., and Nakatani, Y. (1972) Saccharopine dehydrogenase, interaction with substrate analogues. *Eur. J. Biochem. 25*, 301–307.
(27) Xu, H., West, A. H., and Cook, P. F. (2006) Overall kinetic mechanism of saccharopine dehydrogenase from *Saccharomyces cerevisiae*. *Biochemistry 45*, 12156–12166.
(28) Brunhuber, N. M. W., and Blanchard, J. S. (1994) The biochemistry and enzymology of amino acid dehydrogenases. *Crit. Rev. Biochem. Mol. Biol. 29*, 415–467.
(29) Rife, J. E., and Cleland, W. W. (1980) Determination of the chemical mechanism of glutamate dehydrogenase from pH studies. *Biochemistry 19*, 2328–2333.
(30) Meredith, M. J., Gronostajski, R. M., and Schmidt, R. R. (1978) Physical and kinetic properties of the nicotinamide adenine dinucleotide-specific glutamate dehydrogenase purified from *Chlorella sorokiniana*. *Plant Phys. 61*, 967–974.
(31) Grimshaw, C. E., Cook, P. F., and Cleland, W. W. (1981) Use of isotope effects and pH studies to determine the chemical mechanism of *Bacillus subtilis* L-alanine dehydrogenase. *Biochemistry 20*, 5655–5661.
(32) Brunhuber, N. M. W., Thoden, J. B., Blanchard, J. S., and Vanhooke, J. L. (2000) *Rhodococcus* L-phenylalanine dehydrogenase: kinetics, mechanism, and structural basis for catalytic specificity. *Biochemistry 39*, 9174–9187.
(33) Sekimoto, T., MatsuyamaS, T., Fukui, T., and Tanizawa, K. (1993) Evidence for lysine 80 as general base catalyst of leucine dehydrogenase. *J. Biol. Chem. 268*, 27039–27045.
(34) Andi, B., Xu, H., Cook, P. F., and West, A. H. (2007) Crystal structures of ligand-bound saccharopine dehydrogenase from *Saccharomyces cerevisiae*. *Biochemistry 46*, 12512–12521.
(35) Quinn, D. M., and Sutton, L. D. (1991) in Enzyme Mechanism from Isotope Effects (Cook, P. F., Ed.) pp 73−126, CRC Press, Boca Raton, FL.
(36) Dawson, R. M. C., Elliott, D. C., Elliott, W. H., and Jones, K. H. (1991) Data for Biochemical Research , p 130, Oxford University Press, New York.
(37) Karsten, W. E., Lai, C.-J., Gavva, S. R., and Cook, P. F. (1995) Inverse solvent deuterium isotope effects in the NAD-malic enzyme reaction are the result of the viscosity difference between H_2O and D_2O: implications for solvent deuterium isotope effect studies. *J. Am. Chem. Soc. 117*, 5914–5918.
(38) Lin, Y., Volkman, J., Nicholas, K. M., Yamamoto, T., Eguchi, T., Nimmo, S. L., West, A. H., and Cook, P. F. (2008) Chemical mechanism of homoisocitrate dehydrogenase from *Saccharomyces cerevisiae*. *Biochemistry 47*, 4169–4180.
(39) Wong, K. K., and Blanchard, J. S. (1989) Human erythrocyte glutathione reductase: pH dependence of kinetic parameters. *Biochemistry 28*, 3586–3590.